Computers & Geosciences 86 (2016) 46–54

Contents lists available at ScienceDirect

Computers & Geosciences

journal homepage: www.elsevier.com/locate/cageo

Separation of simultaneous sources using a structural-oriented median filter in the flattened dimension

Shuwei Gan [a], Shoudong Wang [a,*], Yangkang Chen [b], Xiaohong Chen [a], Kui Xiang [a]

[a] State Key Laboratory of Petroleum Resources and Prospecting, China University of Petroleum, Fuxue Road 18th, Beijing 102200, China
[b] Bureau of Economic Geology, Jackson School of Geosciences, The University of Texas at Austin, University Station, Box X, Austin, TX 78713-8924, USA

ARTICLE INFO

Article history:
Received 17 April 2015
Received in revised form
23 September 2015
Accepted 1 October 2015
Available online 13 October 2015

Keywords:
Simultaneous sources
Structural-oriented median filter
Plane-wave destruction
Velocity slope transformation

ABSTRACT

Simultaneous-source shooting can help tremendously shorten the acquisition period and improve the quality of seismic data for better subsalt seismic imaging, but at the expense of introducing strong interference (blending noise) to the acquired seismic data. We propose to use a structural-oriented median filter to attenuate the blending noise along the structural direction of seismic profiles. The principle of the proposed approach is to first flatten the seismic record in local spatial windows and then to apply a traditional median filter (MF) to the third flattened dimension. The key component of the proposed approach is the estimation of the local slope, which can be calculated by first scanning the NMO velocity and then transferring the velocity to the local slope. Both synthetic and field data examples show that the proposed approach can successfully separate the simultaneous-source data into individual sources. We provide an open-source toy example to better demonstratethe proposed methodology.

1. Introduction

Wide-azimuth acquisition geometry can improve the illumination of subsalt structures, which helps improve the quality of seismic imaging. However, wide-azimuth acquisition suffers from the low-efficiency problem, resulting from the large temporal shooting interval between two consecutive shots. The large temporal shooting interval is needed to ensure that no interference exists between adjacent shots. The principal purpose of simultaneous source acquisition is to accelerate the acquisition of a larger-density seismic dataset that allows the temporal or spatial overlap between different shots, which saves numerous acquisition cost and increases data quality. The improved seismic data with denser spatial sampling can also help improve the seismic imaging quality of the subsalt structure. The benefits of the new technique are compromised by the intense interference between different shots (Berkhout, 2008). One way for solving the problem caused by interference is by first-separating and second-processing strategy (Chen et al., 2014a), which is also called deblending (Akerberg et al., 2008; Abma et al., 2010; Huo et al., 2012; Mahdad et al., 2011, 2012; Blacquiere and Mahdad, 2012; Beasley et al., 2012; Doulgeris et al., 2012; Bagaini et al., 2012; Li et al., 2013; Ibrahim and Sacchi, 2014; Chen and Ma, 2014; Chen et al., 2014b; Berkhout and Blacquiere, 2014; Chen, 2014, 2015; Qu et al., 2015; Zu et al., 2015). Another way is by direct imaging and inversion of the blended data by attenuating the interference during inversion process (Verschuur and Berkhout, 2011; Dai and Schuster, 2011; Xue et al., 2014; Chen et al., 2015b; Gan et al., 2014). Currently, deblending is still the dominant way for dealing with simultaneous-source data.

There are generally two types of deblending approaches that have been reported in the literature: (1) treating deblending as a noise attenuation approach (Huo et al., 2012; Chen and Ma, 2014; Chen et al., 2014b; Chen, 2014; Chen and Fomel, 2014, 2015), (2) treating deblending as an inversion problem (Mahdad et al., 2011; Abma et al., 2010; Chen et al., 2014a; Gan et al., 2015b). For the filtering based approaches, most of the approaches are based on a median filter. Chen et al. (2014b) proposed to use a common midpoint domain for deblending, because of the better coherency of useful signals and also because the near-offset useful events follow the hyperbolic assumption and thus can be flattened using normal moveout (NMO) correction. A simple median filtering (MF) can be applied to the NMO corrected common-midpoint (CMP) gathers to attenuate blending noise. Chen (2014) proposed a type of MF with spatially varying window length. The space-varying median filter (SVMF) does not require the events to be flattened and is also better applied in the midpoint domain. Huo et al. (2012) used a multidirectional vector median filter after resorting the data into common midpoint gathers. For inversion based approaches, because of the ill-posed property of the inversion problem, there should be some constraint to regularize the inversion

* Corresponding author.
E-mail addresses: gsw19900128@126.com (S. Gan), wangshoudong@163.com (S. Wang), ykchen@utexas.edu (Y. Chen), chenxh@cup.edu.cn (X. Chen), xiangkui15@126.com (K. Xiang).

http://dx.doi.org/10.1016/j.cageo.2015.10.001
0098-3004/

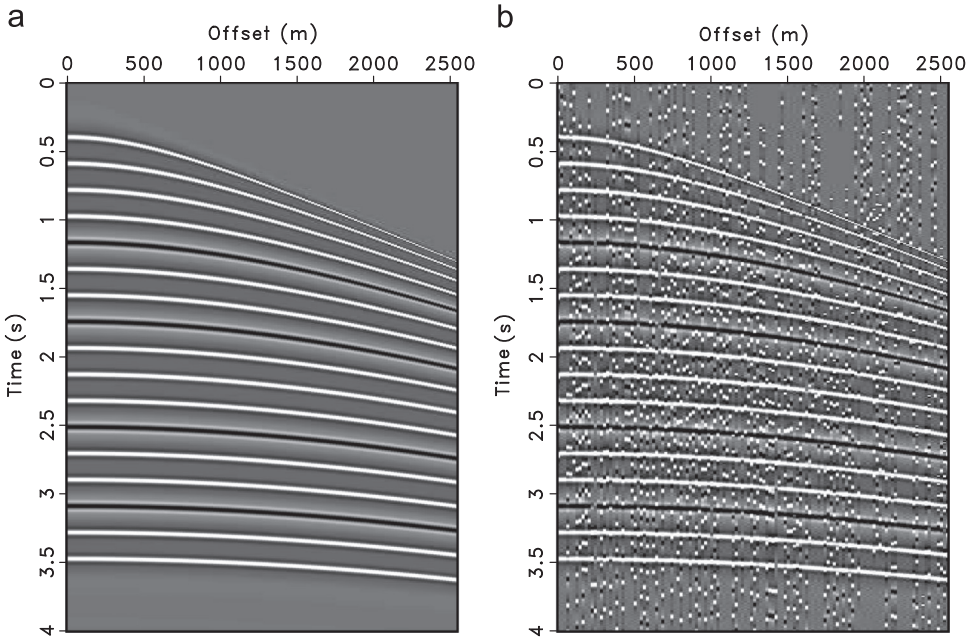

Fig. 1. Synthetic example in common midpoint domain. (a) Unblended data. (b) Blended data.

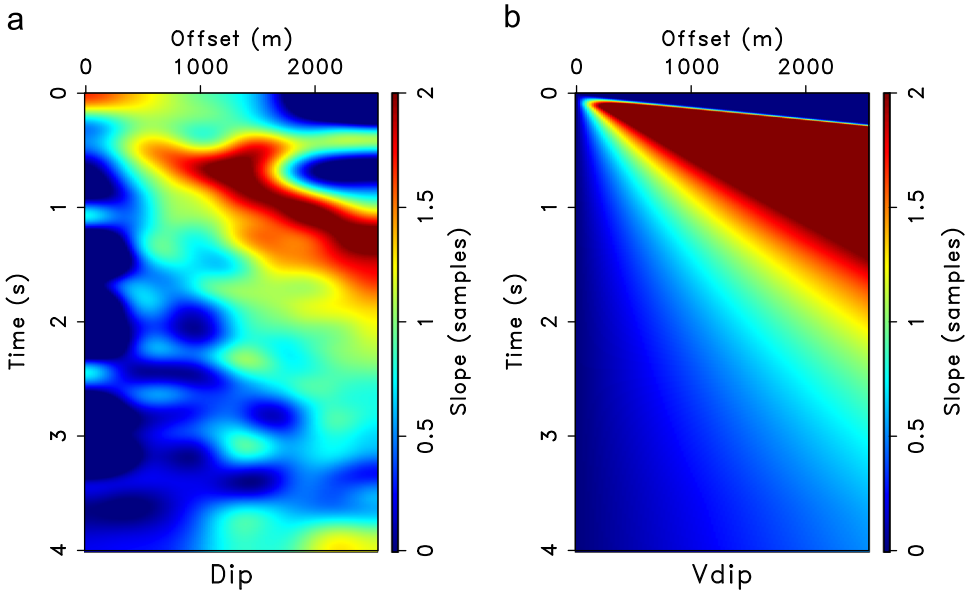

Fig. 2. Local slope maps using (a) PWD, (b) velocity-slope transformation.

problem. Akerberg et al. (2008) used sparsity constraint in the Radon domain to regularize the inversion. A sparsity constraint was also used by Abma et al. (2010) to minimize the energy of incoherent events present in blended data. Lin and Herrmann (2009) connected a curvelet-based sparse inversion algorithm with the emerging field of compressive sensing. Bagaini et al. (2012) compared two separation techniques for the dithered slip-sweep (DSS) data using the sparse inversion method and f–x predictive filtering (Canales, 1984), and pointed out the advantage of the inversion methods over the filtering based approaches. In order to deal with the aliasing problem, Beasley et al. (2012) proposed the alternating projection method (APM), which chooses corrective projections to exploit data characteristics and is claimed to be less sensitive to aliasing than alternative approaches. Mahdad and Blacquiere (2010) proposed a coherence-based inversion approach to deblending of the simultaneous-source data. The convergence properties and the algorithmic aspects of the method were discussed by Doulgeris et al. (2012) and Mahdad et al. (2012), respectively. Although the inversion-based approaches have been demonstrated to obtain better deblending performance (Bagaini et al., 2012), it usually takes many iterations to process the data. Currently, the most efficient way for deblending is using some types of median filtering. However, most of the median filtering approaches are directly borrowed from the signal-processing field and do not utilize the structure information of seismic data.

In this paper, we propose a novel type of MF that makes use of the structural features of seismic data by means of first flattening the seismic record in local spatial windows and then applying MF along the flattened dimension. The flattening operator is constructed by predicting the neighbor traces following the local slope. One concern for such flattening processing is the estimation of an accurate-enough local slope map, which can be solved by first scanning the NMO velocity and then transferring the velocity to the local slope in the common midpoint domain. We first

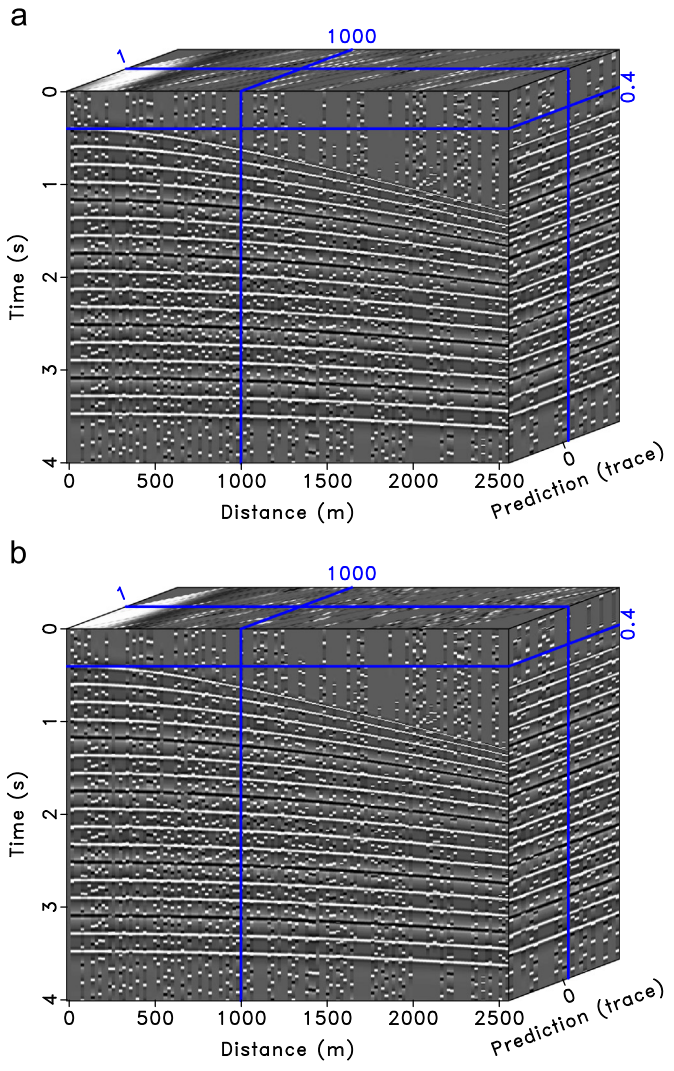

Fig. 3. Flattened domain of the blended data. The MF is to be applied along the third dimension of the cube. (a) From the slope map using PWD. (b) From the slope map using velocity-slope transformation.

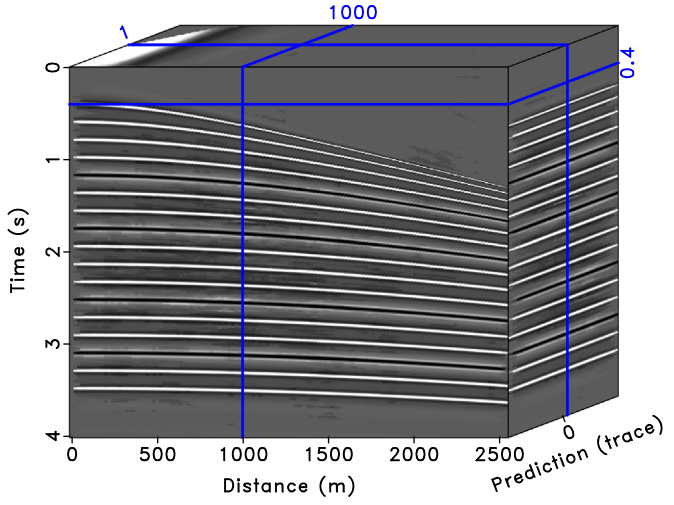

Fig. 4. Flattened domain of the blended data after MF.

review the principle of separating simultaneous sources (deblending) and then introduce the theory of both traditional MF and the proposed structural-oriented median filter (SOMF). Next, we introduce the method of transferring the NMO velocity to local slope in the common midpoint domain. Finally, we use two synthetic examples and one simulated field data example to demonstrate the separating performance of the proposed approach.

2. Method

2.1. Deblending of simultaneous-source data

In a simultaneous-source acquisition, more than one source are blended onto one constant receiver record:

$$\mathbf{d} = \Gamma\mathbf{m}, \tag{1}$$

where $\mathbf{d}$ is the blended data, $\mathbf{m}$ is the unblended data, and Γ denotes the blending operator (Mahdad et al., 2011; Chen et al., 2014a, 2015a). The principal issue in simultaneous-source acquisition is to separate the blended sources into individual sources as if they were acquired independently, which also corresponds to solving Eq. (1) for $\mathbf{m}$.

The simplest way to approximate $\mathbf{m}$ is called the pseudo-deblending:

$$\hat{\mathbf{m}} = \Gamma^{*}\mathbf{d}. \tag{2}$$

Eq. (2) corresponds to arranging the seismic records according to the shot schedules of each source in a common receiver gather, which honors the coherency between different shots in each source and makes the interference from other sources randomly spread the receiver domain. The inversion problem as shown in Eq. (1) is then transformed to be a noise attenuation problem that separates the spatially coherent signals from the random interference.

A more accurate but also time-consuming approach for solving Eq. (1) is to use iterative solver to invert $\mathbf{m}$ with some constraints. One of the currently popular and effective ways is to use a POCS like solver with a transformed domain sparse constraint (Abma et al., 2010; Chen et al., 2014a; Gan et al., 2015c, 2015d):

$$\mathbf{m}_{n+1} = \mathbf{A}^{-1}\mathbf{T}\mathbf{A}[\mathbf{m}_n + \lambda\Gamma^{*}(\mathbf{d} - \Gamma\mathbf{m}_n)], \tag{3}$$

where $\mathbf{m}_n$ is the inverted solution after nth iterations, $\mathbf{A}$ and $\mathbf{A}^{-1}$ denote the forward and inverse sparse transforms respectively, $\mathbf{T}$ denotes a thresholding operator, and λ denotes the step size of the model update. The Fourier transform, the curvelet transform, the Radon transform, and the seislet transform are the currently popular sparse transforms for deblending.

The performance of deblending heavily depends on the sparsity of the selected sparse transform. However, most sparse transforms are model dependent, which means that the transforms are based on some assumptions about the data structure. As we know, the seismic data is highly non-stationary and the commonly used sparse transforms cannot obtain acceptable level of sparsity, which will result in non-optimal inversion performance. What is even worse is that the inversion may not be stable when blending interference is too strong or the sparse transform domain is not sparse enough. Even though we can use inversion based deblending approach to obtain satisfactory results, the deblending process will take a large number of iterations. Considering the modern seismic acquisition is becoming amazingly larger and larger, the iterative inversion is very time consuming. In the next sections, we will propose a non-iterative deblending approach based on median filtering, which is of exceptional convenience for removing the blending interference.

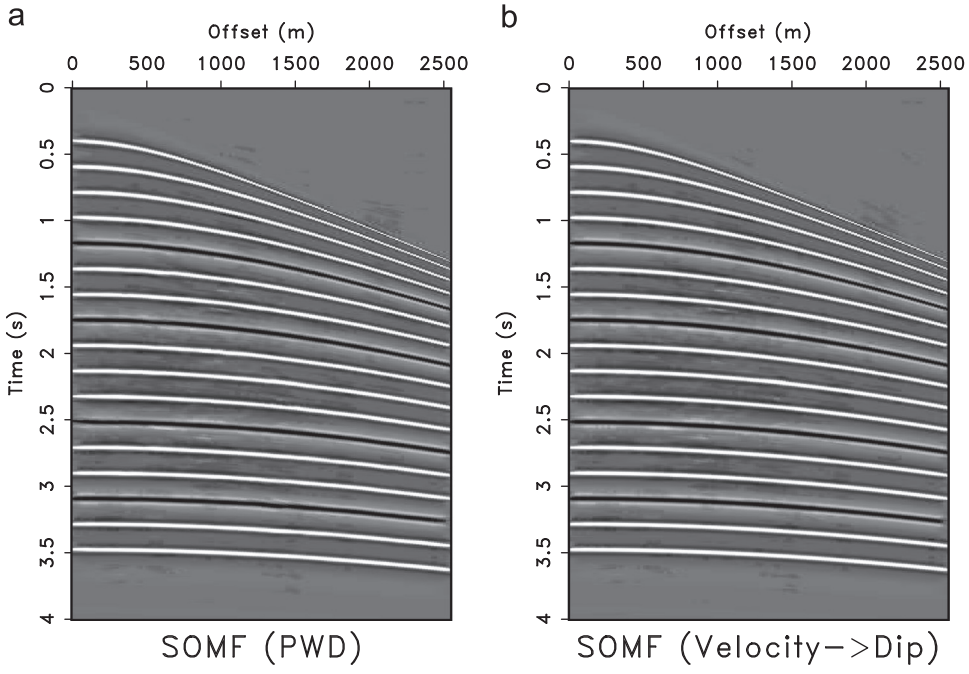

Fig. 5. Deblended results using slopes from (a) PWD, (b) velocity-slope transformation.

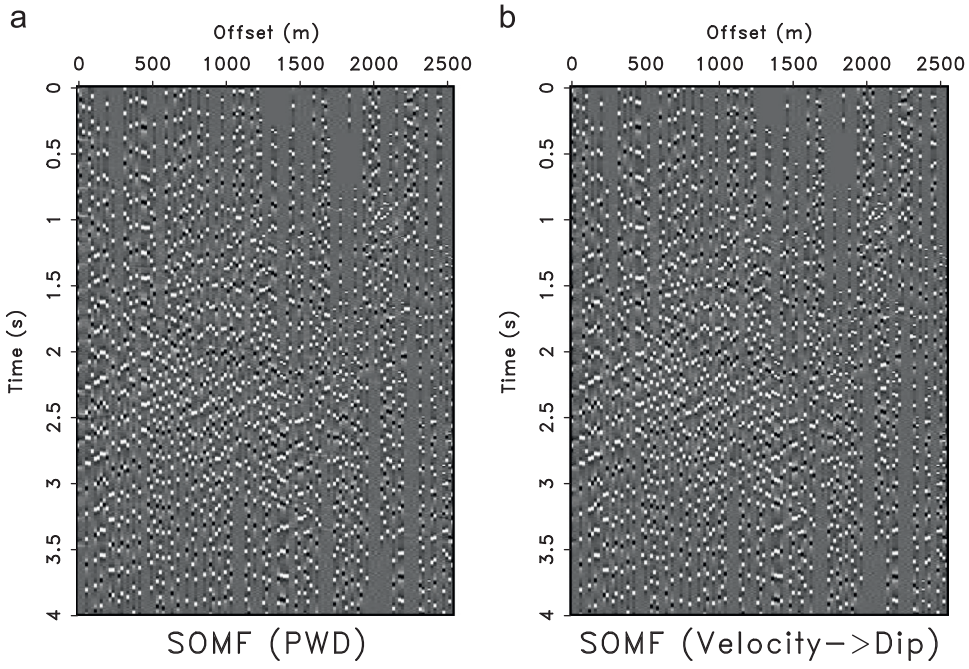

Fig. 6. Blending noise sections using slopes from (a) PWD, (b) velocity-slope transformation.

2.2. Median filtering

The MF is commonly used to remove spiky noise in signal-processing field. For the purpose of removing spiky noise in seismic data, the MF is applied point by point. For each point in the seismic data, we choose a local window that centers at the current point and then pick the median of the local window to be the final value of the current point. The basics of finding the median of a local window is to solve the following minimization problem:

$$\hat{u}_{i,j} = \arg \min_{u_m \in U_{i,j}} \sum_{l=1}^{L} \|u_m - u_l\|_p, \tag{4}$$

where $\hat{u}_{i,j}$ is the output value for location $x_{i,j}$, $U_{i,j} = \{u_1, u_2, \ldots, u_L\}$, i, j are the position indices in a 2-D profile, and l and m are both indices in the filtering window. L is the length of the filtering window, and p denotes L_p norm. Commonly $p=1$ corresponds to standard MF.

Because the blending noise caused from the simultaneous shooting is spike-like along the spatial direction, we can use the MF to effectively remove it. However, the traditional MF is only applicable to those seismic data that mainly composed of horizontal reflections, otherwise much useful reflection energy will be damaged. Thus, we need to either find a way to flatten the seismic data or apply the MF along the structural direction.

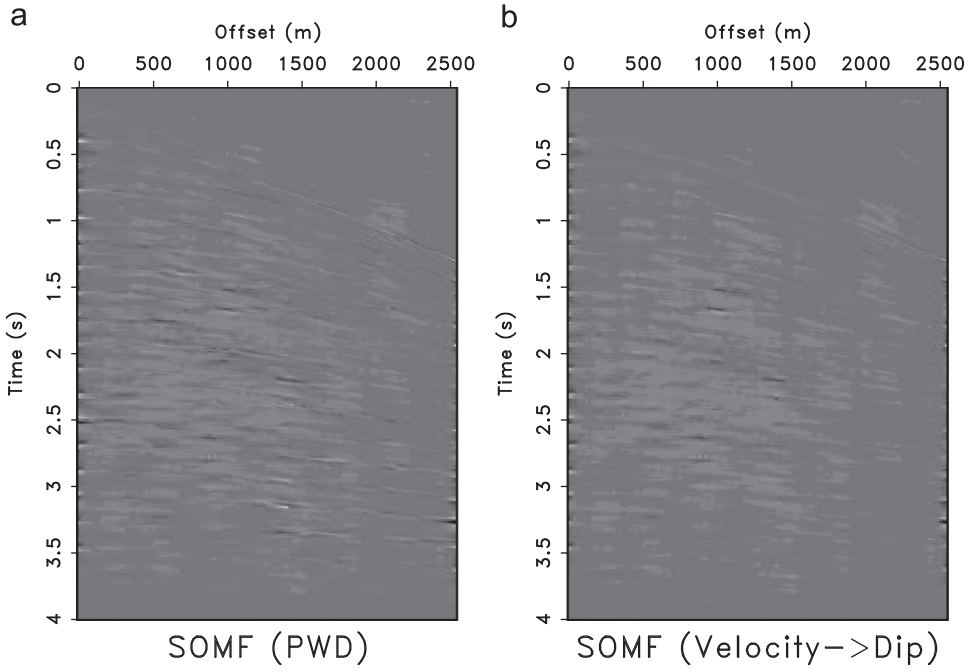

Fig. 7. Deblending error sections using slopes from (a) PWD, (b) velocity-slope transformation.

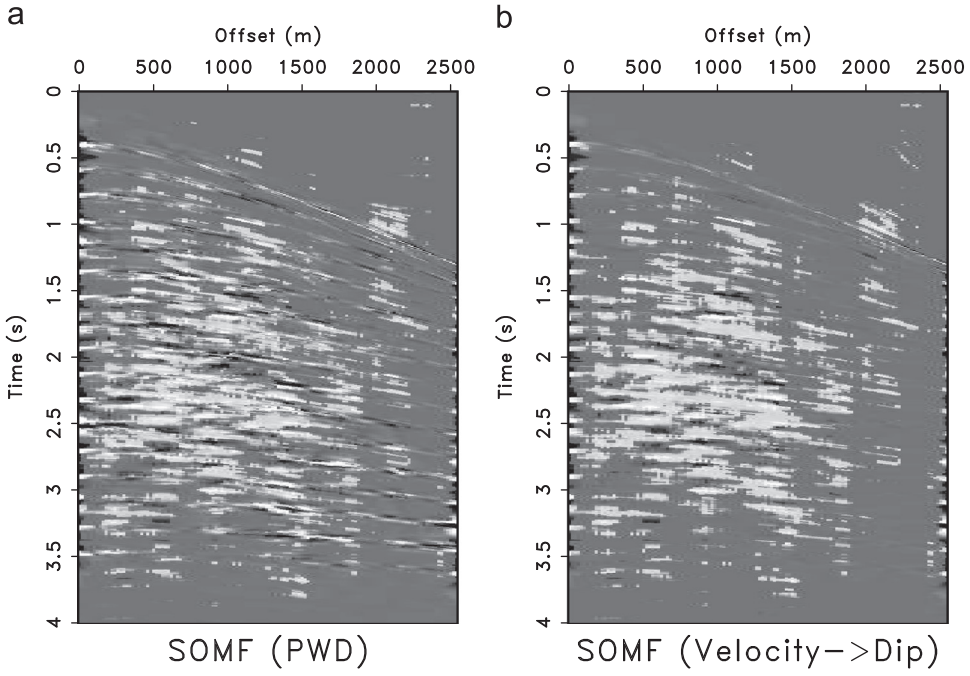

Fig. 8. Amplified deblending error sections (×5) using slopes from (a) PWD, (b) velocity-slope transformation.

2.3. Structural-oriented median filtering

We propose a type of median filter that is applied along the local structure to remove the blending interference. The principle of the approach is to first flatten the seismic data in a local spatial window:

$$\mathbf{P}_j\mathbf{D}_j^R = \overline{\mathbf{D}}_j^R. \tag{5}$$

where $\mathbf{P}_j$ is the jth flattening operator, and j corresponds to the jth trace. And then, we apply a traditional median filter along the flattened direction. Here, the flattening operator is chosen as a plane-wave prediction operator related with the local slope. $\mathbf{D}_j^R$ denotes the jth spatial window (corresponding to jth trace) with a radius of R, $\overline{\mathbf{D}}_j^R$ denotes the flattened local spatial window. Eq. (5) has the following detailed form (Gan et al., 2015a):

$$\begin{bmatrix} \mathbf{P}_{(1,j)\to(1+R,j)}(\sigma_{1,j}) & & \\ & \ddots & \\ & & \mathbf{P}_{(1+2R,j)\to(1+R,j)}(\sigma_{1+2R,j}) \end{bmatrix}$$

$$[\mathbf{d}_{1,j}, \ldots, \mathbf{d}_{1+R,j}, \ldots, \mathbf{d}_{1+2R,j}] = [\overline{\mathbf{d}}_{1,j}, \ldots, \overline{\mathbf{d}}_{1+R,j}, \ldots, \overline{\mathbf{d}}_{1+2R,j}]. \tag{6}$$

Here, $\mathbf{P}_{(i,j)\to(k,j)}(\sigma_{i,j})$ denotes the prediction operator from trace i to trace k in jth spatial window, which is connected with the local

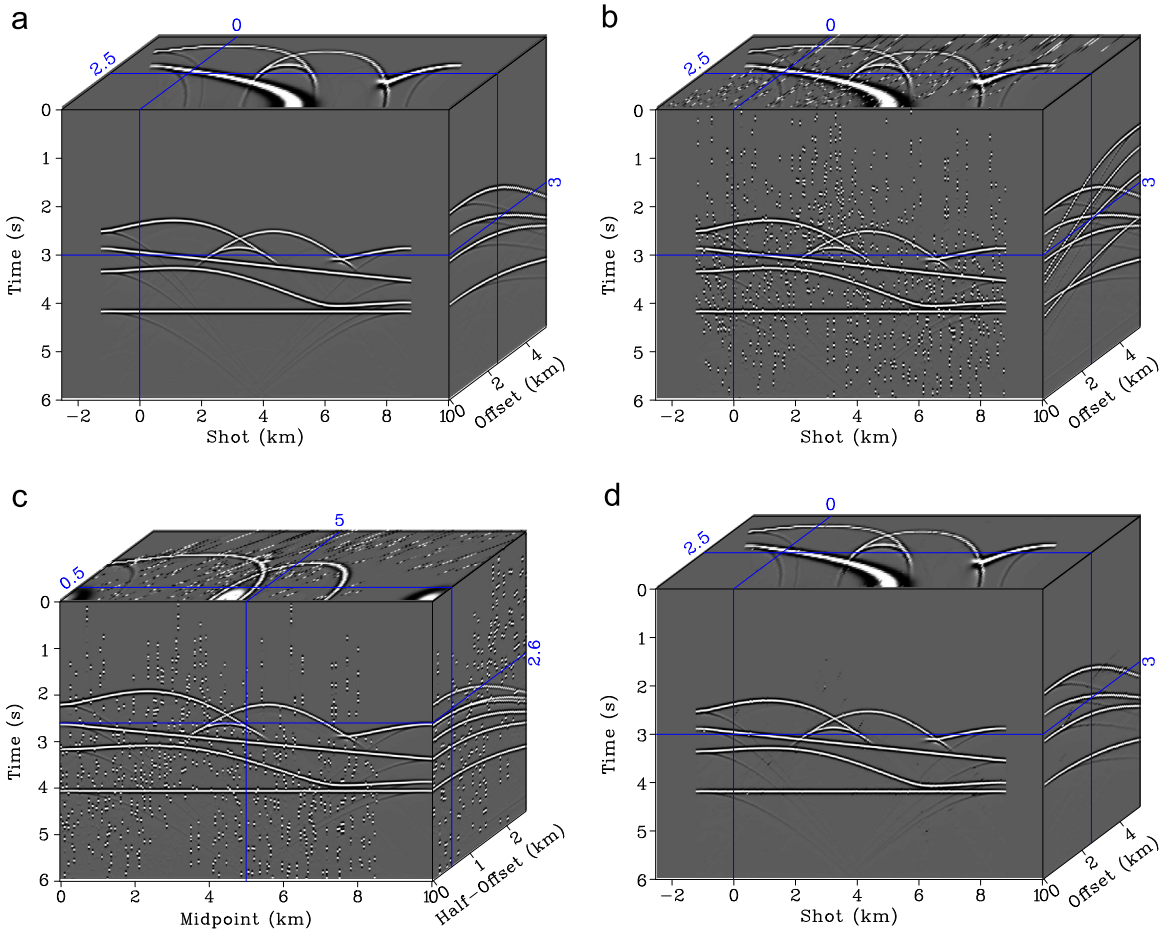

Fig. 9. Pre-stack synthetic example. (a) Unblended data in shot domain. (b) Blended data in shot domain. (c) Blended data in midpoint domain. (d) Deblended data in shot domain.

slope of ith trace $\sigma_{i,j}$. $\mathbf{d}_{i,j}$ denotes the ith trace in the jth spatial window. $\overline{\mathbf{d}}_{i,j}$ denotes the ith trace in the jth spatial window after flattening. Prediction of a trace consists of shifting the original trace along dominant event slopes (Fomel, 2010). Prediction of a trace from a distant neighbor can be accomplished by simple recursion (Liu and Fomel, 2010), i.e., predicting trace k from trace 1 is simply

$$\mathbf{P}_{(1,j)\to(k,j)}(\sigma_{1,j}) = \mathbf{P}_{(k-1,j)\to(k,j)}(\sigma_{k-1,j})\ldots\mathbf{P}_{(2,j)\to(3,j)}(\sigma_{2,j})\mathbf{P}_{(1,j)\to(2,j)}(\sigma_{1,j}). \quad (7)$$

The dominant slopes are estimated by solving the following least-square minimization problem using regularized least-squares optimization:

$$\hat{\sigma} = \arg\min_{\sigma} \|\mathbf{W}(\sigma)\mathbf{D}\|_2^2, \quad (8)$$

where $\mathbf{W}$ is the destruction operator defined as

$$\mathbf{W} = \begin{bmatrix} \mathbf{I} & 0 & 0 & \cdots & 0 \\ -\mathcal{P}_{1\to 2} & \mathbf{I} & 0 & \cdots & 0 \\ 0 & -\mathcal{P}_{2\to 3} & \mathbf{I} & \cdots & 0 \\ \cdots & \cdots & \cdots & \cdots & \cdots \\ 0 & 0 & \cdots & -\mathcal{P}_{N-1\to N} & \mathbf{I} \end{bmatrix},$$

where $\mathbf{I}$ stands for the identity operator, and $\mathcal{P}_{i\to k}$ describes prediction of trace k from trace i (same as the previous version $\mathbf{P}_{(i,j)\to(k,j)}(\sigma_{i,j})$ except for not in a specific spatial window). The optimization approach as shown in Eq. (8) for obtaining local slope estimation is called plane wave destruction (PWD) (Fomel, 2002).

For each trace, we apply the aforementioned flattening, and then we can obtain a 3D cube of the flattened domain. The final filtered result is obtained by selecting the middle slice in the added third dimension after applying median filtering.

2.4. Estimating local slope from velocity analysis

The local slope estimation in highly noisy blended data is challenging. Instead of directly estimating the local slope using the PWD algorithm, we can alternatively first calculate the NMO velocity using simple NMO-correction based velocity analysis and transform the NMO velocity to local slope (Liu and Liu, 2013) by using

$$p(t, x) = \frac{x}{t(x)v_n^2(t_0, x)}, \quad (9)$$

where t_0 is the zero-offset traveltime, $t(x)$ is the traveltime recorded at offset x, $v_n(t_0, x)$ is the NMO velocity, and $p(t, x) = dt/dx$ is the local slope. The detailed introduction of the velocity to slope transformation was introduced in Liu and Liu (2013).

3. Examples

The first example is a simulated synthetic example. The data has been sorted into the common midpoint domain. Fig. 1a and b shows the unblended and blended data, respectively. By using the direct slope estimation using the PWD algorithm and the velocity-slope transformation, we can obtain two dramatically different

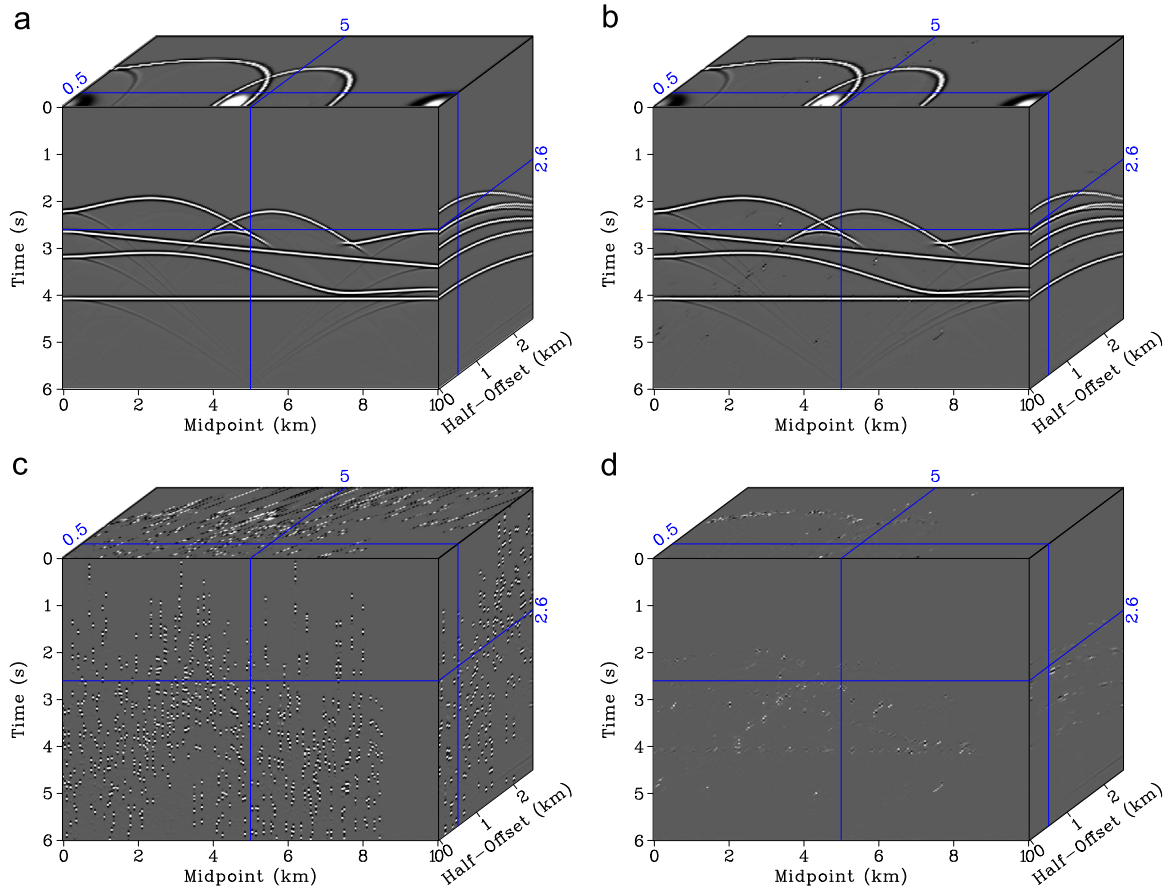

Fig. 10. Pre-stack synthetic example. (a) Unblended data in midpoint domain. (b) Deblended data in midpoint domain. (c) Blending noise in midpoint domain. (d) Deblending error in midpoint domain.

local slope estimations, as shown in Fig. 2. It is obvious that the velocity-slope transformation can obtain much better slope estimation. Figs. 3b and 4 show the 3D cubes of the flattened domain for blended and deblended data, respectively, using the local slope map from the velocity-slope transformation. Fig. 3a shows the flattened blended data that uses the slope map from the PWD algorithm. Fig. 3a and b is very similar, which demonstrates the fact that the flattening process is not very sensitive to the estimated slope. A traditional MF is applied along the third dimension of the 3D cube as shown in Fig. 3b. Fig. 5a and b shows the final deblended data using the two slopes from PWD and velocity-slope estimation, respectively. Both deblended results are very successful because all the blending noise has been removed and there is no obvious damage in the useful energy. We can further confirm the performance by comparing the blending noise sections (Fig. 6) and the deblending error sections (Fig. 7). We also amplified the error sections (Fig. 8) in order to better compare the difference. From Figs. 7 and 8, we can conclude that both deblended results are very similar to the unblended data and the deblended data using the slope from velocity-slope transformation has smaller deblending error. We provide a Python script that can regenerate all the figures (from Figs. 1 to 8) of the first example. From this example, we can see that the two slope estimation approaches will generate similar flattened events and will generate similar deblended results. Thus, the proposed structural-oriented median filter might obtain robust deblending performance even when the slope estimation is not very accurate. It should also be mentioned that though the proposed algorithm is relatively robust, it still depends on an acceptable estimation of the local slope. In the case of extremely strong blending noise, even with the slope–slope transformation we cannot obtain good slope estimation, preliminary processing steps are required to obtain an acceptable slope estimation. The Python script (SConstruct) should be run in the Madagascar open-source environment (Fomel et al., 2013), which can be downloaded at www.ahay.org.

The second example is a simulated pre-stack example. The unblended 3D data cube is shown in Fig. 9a. There are 1501 time samples in this synthetic example and the temporal sampling is 4 ms. The peak frequency is 10 Hz. There are 251 shots and 51 receivers in this example. The shot and receiver intervals are both 50 m. We simulate the blending geometry by using two sources shooting at the two sides of a towed-streamer. Both of the two sources shoot arbitrarilywith a small random dithering. The simulated blended shooting causes strong interference to the data as shown in Fig. 9b. It is apparent that the blending noise appears coherent in common shot gathers and appears random in common offset gathers. By sorting the shot domain (Fig. 9b) to the midpoint domain (Fig. 9c), we can observe that the blending noise appears random in both common offset gathers and common midpoint gathers. The deblending procedures using the proposed approach are applied to Fig. 9c. The detailed deblending comparison is provided in Fig. 10. Fig. 9d shows the final deblended result that is sorted back to the shot domain. We can conclude a successful separation considering the high similarity between Fig. 9a and d. In Fig. 10, we compare the unblended and deblended data in the midpoint domain in (a) and (b), and show the removed the blending noise cube and deblending error cube in (c) and (d), respectively. From the very clean deblended data, incoherent blending noise, and small deblending error, we can further confirm that the proposed approach obtain a successful separation between the signals and interference.

The third example is a simulated field data example. Fig. 11a

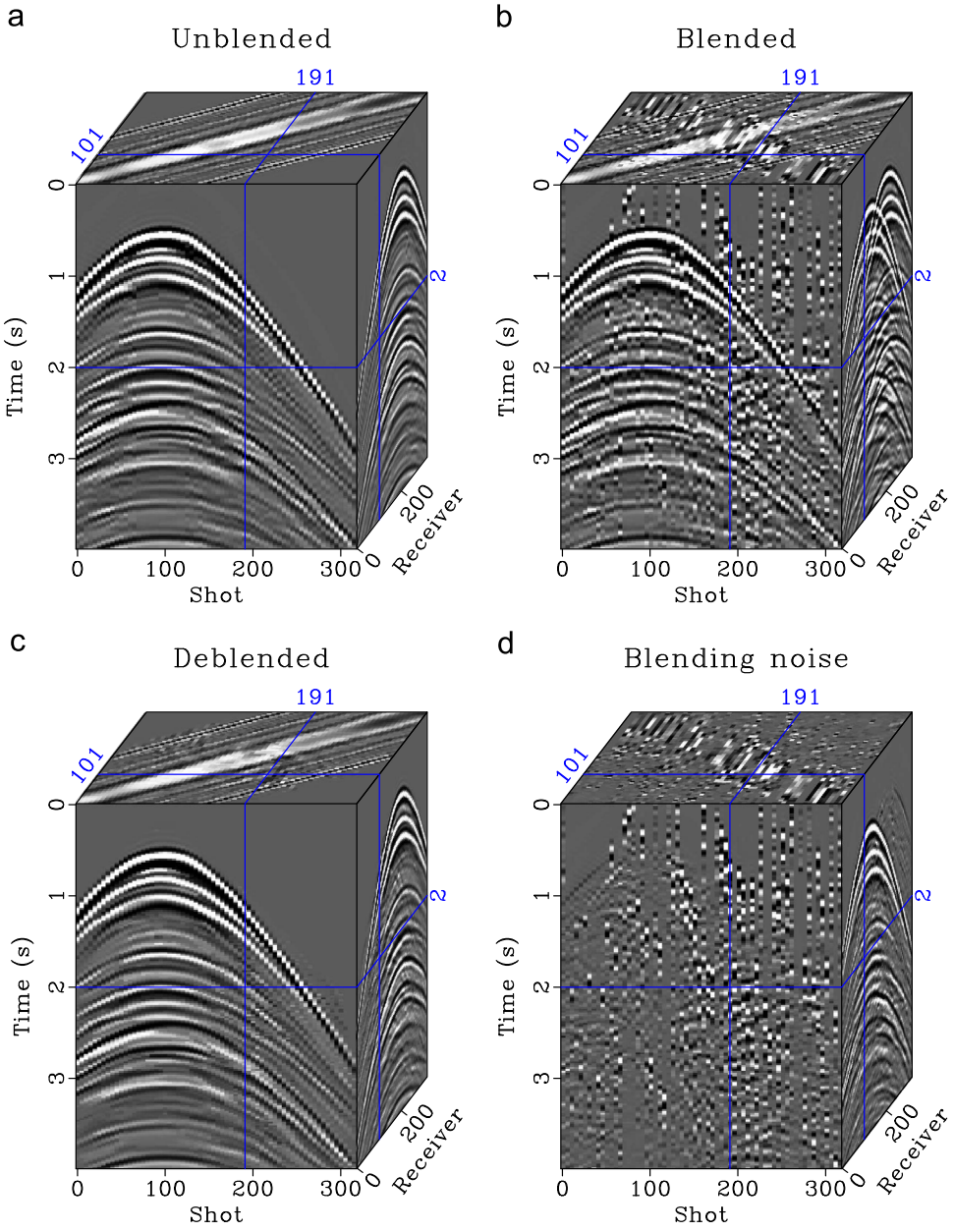

Fig. 11. Field data example. (a) Unblended data. (b) Blended data. (c) Deblended data. (d) Blending noise.

shows the unblended data from a constant-receiver 2D marine survey. Fig. 11b shows the blended data. As we can see, the blending interference appears incoherent in common receiver gathers and coherent in common shot gathers. Fig. 11c shows the deblended result using the proposed approach and (d) shows the blending noise cube. It is obvious that the blending noise in each common receiver gather does not contain coherent reflections and the blending noise appears as coherent source when observed along the third dimension. As we can see, we can use the proposed approach to obtain a nearly perfect separation of simultaneous sources.

4. Conclusion

We have proposed a novel deblending approach using a structural oriented median filter. The proposed median filter is applied in a pre-flattened third dimension of the original data. We use prediction operator following the local slope to flatten the seismic record in local spatial windows. The key aspect in the flattening process is the estimation of the local slope from the highly noisy blended data. Instead of directly estimating the local slope using the PWD algorithm, we can use the velocity-slope transformation to alternatively estimate the slope. While the slope estimation from the PWD algorithm can help obtain acceptable deblending performance, the slope from velocity-slope transformation can help obtain even better performance. Both synthetic and field data examples show successful deblending performance using the proposed approach.

Acknowledgments

We would like to thank Shan Qu, Shaohuan Zu, Zhaoyu Jin, and Jiang Yuan for helpful discussions on the topics of deblending. We

also thank the chief editor Jef Caers and four anonymous reviewers for suggestions that improve the manuscript greatly. This research is supported by the National Natural Science Foundation of China (Grant no. 41274137), the National Science and Technology of Major Projects of China (Grant no. 2011ZX05019-006), and National Engineering Laboratory of Offshore Oil Exploration.

Appendix A. Supplementary data

Supplementary data associated with this article can be found in the online version at http://dx.doi.org/10.1016/j.cageo.2015.10.001.

References

Abma, R.L., Manning, T., Tanis, M., Yu, J., Foster, M., 2010. High quality separation of simultaneous sources by sparse inversion. In: 72nd Annual International Conference and Exhibition, EAGE, Extended Abstracts.

Akerberg, P., Hampson, G., Rickett, J., Martin, H., Cole, J., 2008. Simultaneous source separation by sparse radon transform. In: 78th Annual International Meeting, SEG, Expanded Abstracts, pp. 2801–2805.

Bagaini, C., Daly, M., Moore, I., 2012. The acquisition and processing of dithered slip-sweep vibroseis data. Geophys. Prospect. 60, 618–639.

Beasley, C.J., Dragoset, B., Salama, A., 2012. A 3d simultaneous source field test processed using alternating projections: a new active separation method. Geophys. Prospect. 60, 591–601.

Berkhout, A.J., 2008. Changing the mindset in seismic data acquisition. Lead. Edge 27, 924–938.

Berkhout, A.J., Blacquiere, G., 2014. Combining deblending with multi-level source deghosting. In: 84th Annual International Meeting, SEG, Expanded Abstracts, pp. 41–45.

Blacquiere, G., Mahdad, A., 2012. Deblending of dispersed source array data. In: 82nd Annual International Meeting, SEG, Expanded Abstracts, http://dx.doi.org/10.1190/segam2012-0303.1.

Canales, L., 1984. Random noise reduction. In: 54th Annual International Meeting, SEG, Expanded Abstracts, pp. 525–527.

Chen, Y., 2014, Deblending using a space-varying median filter. Explor. Geophys., http://dx.doi.org/10.1071/EG14051.

Chen, 2015, Iterative deblending with multiple constraints based on shaping regularization. IEEE Geosci. Remote Sens. Lett., http://dx.doi.org/10.1109/LGRS.2015.2463815.

Chen, Y., Fomel, S., 2014. Random noise attenuation using local similarity. In: 84th Annual international meeting, SEG, Expanded Abstracts, pp. 4360–4365.

Chen, Y., Fomel, S., 2015. Random noise attenuation using local signal-and-noise orthogonalization. Geophysics 80, WD1–WD9.

Chen, Y., Fomel, S., Hu, J., 2014a. Iterative deblending of simultaneous-source seismic data using seislet-domain shaping regularization. Geophysics 79, V179–V189.

Chen, Y., Jin, Z., Gan, S., Yang, W., Xiang, K., Bai, M., Huang, W., 2015a. Iterative deblending using shaping regularization with a combined PNMO-MF-FK coherency filter. J. Appl. Geophys. 122, 18–27.

Chen, Y., Ma, J., 2014. Random noise attenuation by *f-x* empirical mode decomposition predictive filtering. Geophysics 79, V81–V91.

Chen, Y., Yuan, J., Jin, Z., Chen, K., Zhang, L., 2014b. Deblending using normal moveout and median filtering in common-midpoint gathers. J. Geophys. Eng. 11, 045012.

Chen, Y., Yuan, J., Zu, S., Qu, S., Gan, S., 2015b. Seismic imaging of simultaneous-source data using constrained least-squares reverse time migration. J. Appl. Geophys. 114, 32–35.

Dai, W., Schuster, G.T., 2011. Least-squares migration of multisource data with a deblurring filter. Geophysics 76, R135–R146.

Doulgeris, P., Bube, K., Hampson, G., Blacquiere, G., 2012. Covergence analysis of a coherency-constrained inversion for the separation of blended data. Geophys. Prospect. 60, 769–781.

Fomel, S., 2002. Application of plane-wave destruction filters. Geophysics 67, 1946–1960.

Fomel, S., 2010. Predictive painting of 3-d seismic volumes. Geophysics 75, A25–A30.

Fomel, S., Sava, P., Vlad, I., Liu, Y., Bashkardin, V., 2013. Madagascar open-source software project. J. Open Res. Softw. 1, e8.

Gan, S., Chen, Y., Qu, S., Liu, T., 2014. Velocity analysis of simultaneous-source data using similarity-weighted semblance. In: 77th Annual International Conference and Exhibition, EAGE, Extended Abstracts, http://dx.doi.org/10.3997/2214-4609.201413050.

Gan, S., Chen, Y., Zu, S., Qu, S., Zhong, W., 2015a. Structure-oriented singular value decomposition for signal enhancement of seismic data. J. Geophys. Eng. 12, 262–272.

Gan, S., Wang, S., Chen, Y., Chen, X., 2015b. Deblending of distance separated simultaneous-source data using seislet frames in the shot domain. In: 85th Annual International Meeting, SEG, Expanded Abstracts, pp. 65–70.

Gan, S., Wang, S., Chen, Y., Chen, X., 2015c. Seismic data reconstruction via fast projection onto convex sets in the seislet transform domain. In: 85th Annual International Meeting, SEG, Expanded Abstracts, pp. 3814–3819.

Gan, S., Wang, S., Chen, Y., Zhang, Y., Jin, Z., 2015d. Dealiased seismic data interpolation using seislet transform with low-frequency constraint. IEEE Geosci. Remote Sens. Lett. 12, 2150–2154.

Huo, S., Luo, Y., Kelamis, P.G., 2012. Simultaneous sources separation via multi-directional vector-median filtering. Geophysics 77, V123–V131.

Ibrahim, A., Sacchi, M.D., 2014. Simultaneous source separation using a robust radon transform. Geophysics 79, V1–V11.

Li, C., Mosher, C.C., Morley, L.C., Ji, Y., Brewer, J.D., 2013. Joint source deblending and reconstruction for seismic data. In: 83rd Annual International Meeting, SEG, Expanded Abstracts, pp. 82–87.

Lin, T.T., Herrmann, F.J., 2009. Designing simultaneous acquisitions with compressive sensing. In: 71st Annual International Conference and Exhibition, EAGE, Extended Abstracts.

Liu, Y., Fomel, S., 2010. Oc-seislet: seislet transform construction with differential offset continuation. Geophysics 75, WB235–WB245.

Liu, Y., Liu, C., 2013. Velocity-dependent seislet transform and its applications. In: 83rd Annual International Meeting, SEG, Expanded Abstracts, pp. 3661–3666.

Mahdad, A., Blacquiere, G., 2010. Iterative deblending of blended encoded shot records. In: 72nd Annual International Conference and Exhibition, EAGE, Extended Abstracts.

Mahdad, A., Doulgeris, P., Blacquiere, G., 2011. Separation of blended data by iterative estimation and subtraction of blending interference noise. Geophysics 76, Q9–Q17.

Mahdad, A., Doulgeris, P., Blacquiere, G., 2012. Iterative method for the separation of blended seismic data: discussion on the algorithmic aspects. Geophys. Prospect. 60, 782–801.

Qu, S., Zhou, H., Chen, Y., Yu, S., Zhang, H., Yuan, J., Yang, Y., Qin, M., 2015. An effective method for reducing harmonic distortion in correlated vibroseis data. J. Appl. Geophys. 115, 120–128.

Verschuur, D.J., Berkhout, A.J., 2011. Seismic migration of blended shot records with surface-related multiple scattering. Geophysics 76, A7–A13.

Xue, Z., Chen, Y., Fomel, S., Sun, J., 2014. Imaging incomplete data and simultaneous-source data using least-squares reverse-time migration with shaping regularization. In: 84th Annual International Meeting, SEG, Expanded Abstracts, pp. 3991–3996.

Zu, S., Zhou, H., Chen, Y., Liu, Y., Qu, S., 2015. A periodically variational dithering code for improving deblending. In: 85th Annual International Meeting, SEG, Expanded Abstracts, pp. 38–42.